Applied Catalysis B: Environmental 158–159 (2014) 314–320

Contents lists available at ScienceDirect

Applied Catalysis B: Environmental

journal homepage: www.elsevier.com/locate/apcatb

Substantial change in phenomenon of "self-corrosion" on Ag_3PO_4/TiO_2 compound photocatalyst

Xinlong Ma[a,1], Huihui Li[a,*,1], Yuhua Wang[a,*], Hao Li[a], Bin Liu[a], Shu Yin[b], Tsugio Sato[b]

[a] Director of the Key Laboratory for Special Function Materials and Structure Design of the Ministry of Education, Lanzhou University, Lanzhou 730000, PR China

[b] Institute of Multidisciplinary Research for Advanced Materials, Tohoku University, 2-1-1 Katahira, Aoba-ku, Sendai 980-8577, Japan

ARTICLE INFO

Article history:
Received 18 January 2014
Received in revised form 16 April 2014
Accepted 19 April 2014
Available online 30 April 2014

Keywords:
Silver orthophosphate
Ag_3PO_4/TiO_2 compound
Photocatalysis
Stability

ABSTRACT

The phenomenon of color-change was first observed in the simple physical mixed Ag_3PO_4/TiO_2 compounds in dark, called "self-corrosion". The difference between self-corrosion and photo-corrosion was clarified. It is found that the chemical environment of Ag is altered in Ag_3PO_4/TiO_2 compounds compared with that in bare Ag_3PO_4. Furthermore, the change in self-corrosion and its impact on photocatalytic activity were investigated. It is found that under ultraviolet (UV) light irradiation the advantage over bare Ag_3PO_4 is still maintained in the self-corrosion Ag_3PO_4/TiO_2 compounds due to the similar adsorption capacity. Meanwhile, the photocatalytic activity of self-corrosion Ag_3PO_4/TiO_2 under visible light irradiation is lower than that of fresh Ag_3PO_4/TiO_2 due to the decrease of Ag_3PO_4. In addition, the identification of oxidative degradation intermediates in the solution was conducted by mass spectra (MS) for the explanation of the degradation mechanism.

1. Introduction

It is well known that semiconductor-based photocatalysts have received great attention as efficient, stable, and environmentally friendly materials in the field of environmental pollution control [1–3]. TiO_2 is one of the most renowned photocatalysts among various semiconductors due to its chemical stability, non-toxicity, low cost and favorable optoelectronic properties [4]. However, TiO_2 cannot take advantage of visible light, which accounts for 45% of solar spectrum, for its large band gap (3.2 eV). Moreover, the low separation rate of the photoexcited electron–hole in TiO_2 leads to limited quantum efficiency, which restricts its practical applications [5,6]. Thus it is necessary and important to develop new and highly efficient visible-light-driven photocatalysts.

Recently, a breakthrough on visible-light-driven photocatalysts was made by Ye et al., who first reported the use of Ag_3PO_4 semiconductor in photocatalytic field, where it exhibited extremely high photooxidative capabilities for the O_2 evolution from water and the decomposition of organic dyes under visible-light irradiation [7–9].

However, it should be noted that the serious stability issue of Ag_3PO_4 photocatalyst is the main hindrance for the practical application of Ag_3PO_4 as a recyclable and highly efficient photocatalyst. Moreover, the conduction band potential of Ag_3PO_4 is more positive than that of the hydrogen potential [10]. Thus, Ag_3PO_4 can absorb a photon to generate an electron and a hole, then, the electron combines with an interstitial silver ion (Ag^+) to give a silver atom, which results in the photo-corrosion of Ag_3PO_4 in the absence of a sacrificial reagent. The appeared black metallic Ag particles would suspend in the photocatalytic reaction systems and attach onto the surface of the Ag_3PO_4 catalyst, which would inevitably prevent the visible light absorption and decrease the photocatalytic activity [11]. More recently, Lee et al. investigated the visible-light photocatalytic behavior of Ag_3PO_4-core/TiO_2-shell composites [12], and Yao et al. reported a facile process to synthesize *in situ* Ag_3PO_4 nanoparticles onto the surface of Degussa P25 TiO_2 photocatalyst particles [13]. Photo-corrosion was not reported in their work since the stability of Ag_3PO_4 is improved. However, the phenomenon of color-change was observed in the simple physical mixed Ag_3PO_4/TiO_2 compounds in dark, called self-corrosion in this work. Therefore, it is an interesting question: what makes the contrary behavior?

In this work, substantial change in phenomenon of self-corrosion on Ag_3PO_4/TiO_2 compound photocatalyst was studied. The difference between self-corrosion and photo-corrosion was clarified. Meanwhile, the change in self-corrosion and its impact on

* Corresponding authors. Tel.: +86 931 8912772; fax: +86 931 8913554; mobile: +86 13919816967.
E-mail addresses: lihh@lzu.edu.cn (H. Li), wyh@lzu.edu.cn (Y. Wang).
[1] Both the authors are co-first authors.

http://dx.doi.org/10.1016/j.apcatb.2014.04.031
0926-3373/

photocatalytic activity were investigated. In addition, the identification of oxidative degradation intermediates in the solution was conducted for the explanation of the degradation mechanism.

2. Experimental

2.1. Sample preparation

Ag_3PO_4 nanoparticles were prepared by ion-exchange reaction between $AgNO_3$ and Na_3PO_4 in solid phase as a reported method [12]. In a typical synthesis, $AgNO_3$ was mixed with stoichiometric amount of Na_3PO_4 and ground in a mortar in dark at ambient condition. After a gentle grinding for about 1 h, the color of the reaction mixture becomes golden. The mixture was then washed with distilled water several times in order to remove the unreacted components and the produced $NaNO_3$. Finally, the golden powders were dried overnight at ambient condition.

The Ag_3PO_4/TiO_2 compounds were prepared by physical mixing the as-prepared Ag_3PO_4 (0.1 g) with various amounts of commercial Degussa P25 TiO_2 particles. The contents of added P25 TiO_2 were 0.50, 0.20, 0.10, and 0.05 g, labeled as 17 wt% Ag_3PO_4/TiO_2, 33 wt% Ag_3PO_4/TiO_2, 50 wt% Ag_3PO_4/TiO_2 and 67 wt% Ag_3PO_4/TiO_2, respectively. It should be pointed out that the above samples were called "fresh" samples and the samples kept for some time in dark were called "self-corrosion" samples labeled as "old samples" in pictures.

2.2. Sample characterization

X-ray diffraction (XRD) experiments were carried out with a D/max-2400 diffractometer (Rigaku, Japan) using Cu-Ka radiation. The morphologies were examined by scanning electron microscopy (SEM, Hitachi S-4800). A FEI Tecnai G2 F30 transmission electron microscope, equipped with a Gatan imaging filter (GIF) system, was used for transmission electron microscopy (TEM). The Brunauer–Emmett–Teller (BET) specific surface area of the samples was measured using a Micromeritics ASAP 2020-M instrument. Diffuse reflectance ultraviolet–visible (UV–vis) absorption spectrum was measured by a PerkinElmer Lambda 950 spectrometer in the region of 200–700 nm, while $BaSO_4$ was used as a reference. X-ray photoelectron spectroscopy (XPS) was conducted on a Kratos AXIS Ultra DLD spectrometer.

2.3. Evaluation of photocatalytic activity

The photocatalytic activity of samples was measured by the decomposition of MB dye in a reactor at room temperature. In a typical process for degradation of a dye, 40 mg of photocatalyst was suspended in the MB dye solution (10 mg/L, 75 mL). Before irradiation, the suspensions were stirred for 30 min in the dark to ensure the establishment of adsorption–desorption equilibrium. A 500 W high-pressure mercury lamp was employed for the UV irradiation source and a 300 W Xe arc lamp equipped with a UV cutoff filter ($\lambda \geq 420$ nm) for the visible light source which was positioned 20 cm away from the reactor to trigger the photocatalytic reaction. A certain volume of suspension were withdrawn at selected times for analysis. After recovering the photocatalyst by centrifugation, the concentration of dye solution was analyzed by measuring the light absorption of the clear solution at 664 nm (λ_{max} for MB solution) using a spectrophotometer (WFJ-7200, Unico, USA). The percentage of degradation was calculated by C/C_0. Here, C is the concentration of remaining dye solution at each irradiated time interval, while C_0 is the initial concentration. The MS were obtained with Bruker Daltonics esquire6000 mass instrument (ESI) for the identification of oxidative degradation intermediates in the dye solution.

To prepare photo-corrosion samples, the cycling runs in photocatalytic degradation of MB dye solution in the presence of photocatalyst were checked. After one cycle, the photocatalyst was filtrated and washed thoroughly with deionized water, and then fresh MB solution (10 mg/L) was added to the photocatalyst to begin the next cycling run. Three consecutive cycles were completed and each cycle lasted for 15 min. The samples after three cycles were called "photo-corrosion" samples labeled as "Rec samples" in pictures.

3. Results and discussion

3.1. Phenomenon of self-corrosion

The phenomenon of color-change was first observed in the simple physical mixed Ag_3PO_4/TiO_2 compounds in dark, called "self-corrosion". Fig. 1(a–c) shows fresh sample pictures of P25 TiO_2, bare Ag_3PO_4 and simple physical mixed Ag_3PO_4/TiO_2 compounds, respectively, and their counterparts kept in dark for 5 days are shown in Fig. 1(d–f). As shown in the top row, the colors are white, golden and yellowish corresponding to P25 TiO_2, bare Ag_3PO_4 and Ag_3PO_4/TiO_2 compounds, respectively. However, as shown in the bottom row, the colors become white, dark yellow and brown. It is noted that the color of Ag_3PO_4/TiO_2 compounds changes from yellowish to brown in dark, called "self-corrosion". Furthermore, this phenomenon of color-change suggests that something changes after simple physical mixing Ag_3PO_4 and P25 TiO_2.

In order to make clear what changes in the phenomenon of color-change (so-called self-corrosion), SEM, TEM, XRD and XPS technologies were employed.

3.2. Substantial change in phenomenon of self-corrosion

Fig. S1(a) (in Supplementary data) shows the distribution of Ag_3PO_4 nanoparticles is non-uniform, and the inset of Fig. S1(a) shows the average particle size taken from statistics analysis by measuring cross diagonals of these Ag_3PO_4 particles, which is about 279 nm. It is also noticed that most of the Ag_3PO_4 particles have a spherical shape. Fig. S1(b) shows SEM image of P25 TiO_2. It can be seen that the particle size of P25 TiO_2 is about 20 nm, which is much smaller than that of bare Ag_3PO_4 particles.

TEM image of self-corrosion 33 wt% Ag_3PO_4/TiO_2 compounds (as typical sample) is depicted in Fig. 2(a). It can be seen that the Ag_3PO_4 particles are surrounded with P25 TiO_2 particles. The specific surface area (S.S.A.) of self-corrosion 33 wt% Ag_3PO_4/TiO_2 (S.S.A. 42.2 m^2/g) is slightly lower than that of P25 TiO_2 particles (S.S.A. 46.2 m^2/g) but far larger than that of Ag_3PO_4 (S.S.A. 1.7 m^2/g), which is in agreement with above TEM result. Moreover, the inset of Fig. 2(a) shows the TEM image of a small region of 33 wt% Ag_3PO_4/TiO_2 compounds, where only P25 TiO_2 particles are observed. It is found that there are some tiny particles on the surface of P25 TiO_2 particles labeled by white cycles. Fig. 2(b) shows the TEM and HRTEM images of bare P25 TiO_2 particles. It can be seen that the particle size of P25 TiO_2 is about 20 nm, and HRTEM image clearly shows the lattice fringes. The lattice spacing is 0.354 nm, corresponding to the (1 0 1) planes of anatase TiO_2.

Thus, XRD is employed to make clear the constitution of the tiny particles. Fig. S2 shows the XRD patterns of self-corrosion 17 wt% Ag_3PO_4/TiO_2, 33 wt% Ag_3PO_4/TiO_2, 50 wt% Ag_3PO_4/TiO_2, 67 wt% Ag_3PO_4/TiO_2 and photo-corrosion 33 wt% Ag_3PO_4/TiO_2, respectively. The XRD patterns of all self-corrosion Ag_3PO_4/TiO_2 compounds show the mixed patterns of the Ag_3PO_4 and TiO_2 phases, which is similar to that of the fresh Ag_3PO_4/TiO_2 compounds (Fig S3). It is noted that the intensity ratio of individual

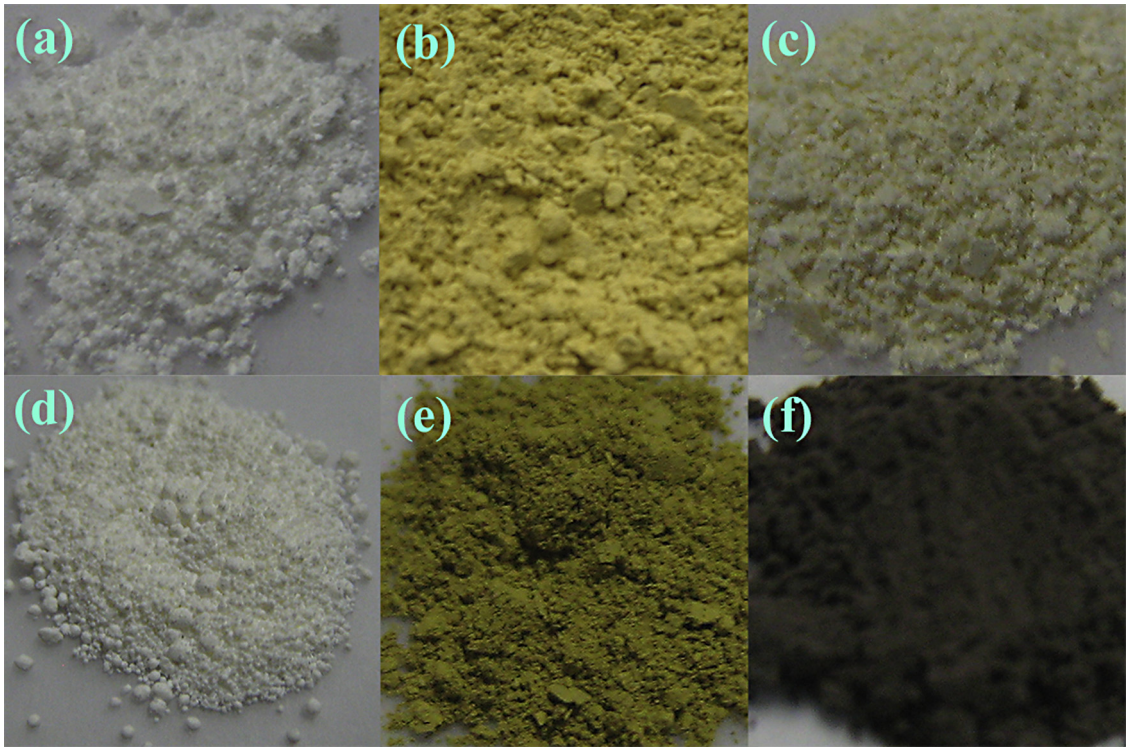

Fig. 1. Pictures of fresh samples of P25 TiO_2, bare Ag_3PO_4 and Ag_3PO_4/TiO_2 compounds (a–c) and their counterparts kept in dark for 5 days (d–f).

peaks is dependent on the percentage of Ag_3PO_4 in Ag_3PO_4/TiO_2 compounds. Meanwhile, no impurity is observed in the self-corrosion samples, neither Ag_2O (JCPDS card numbers 41-1104) nor Ag (JCPDS card numbers 04-0783), due to the much lower amount of the tiny particles. In contrast, it is noted that for the photo-corrosion 33 wt% Ag_3PO_4/TiO_2, diffraction peak at 33.3° disappears and the peak at 44.3° appears corresponding to the absence of Ag_3PO_4 and the formation of Ag.

In order to make this phenomenon clear, XPS spectrum is employed to further analyze the elemental composition and chemical status. As shown in Fig. 3, the two symmetrical peaks at 368.05 and 374.10 eV are corresponded to Ag $3d_{5/2}$ and Ag $3d_{3/2}$ for fresh Ag_3PO_4 sample. These peaks can be attributed to Ag^+ ions in Ag_3PO_4 according to the results reported by Zhang et al. [14] and Liu et al. [15]. Compared with bare Ag_3PO_4, the XPS peaks of Ag at 367.65 and 373.62 eV for self-corrosion 33 wt% Ag_3PO_4/TiO_2 show a slight lower binding energy and a larger full width at half maximum (FWHM). According to the result reported by Arabatzis et al. [16], the slight decrease of binding energy for silver element can be ascribed to the formation of Ag_xO ($x = 1,2$) particle (Ag_2O is partially decomposed into Ag atoms and AgO), which also results in the increase of FWHM. This result is confirmed by the TEM images discussed above. Furthermore, once absorbing incident light, the AgO phase generated by decomposition of Ag_2O can immediately be photoreduced to form metallic Ag and O_2 [17]. As a result, the XPS peak of Ag for photo-corrosion 33 wt% Ag_3PO_4/TiO_2 are shifted between that of fresh Ag_3PO_4 and self-corrosion 33 wt% Ag_3PO_4/TiO_2 and the FWHM decreases compared with that of

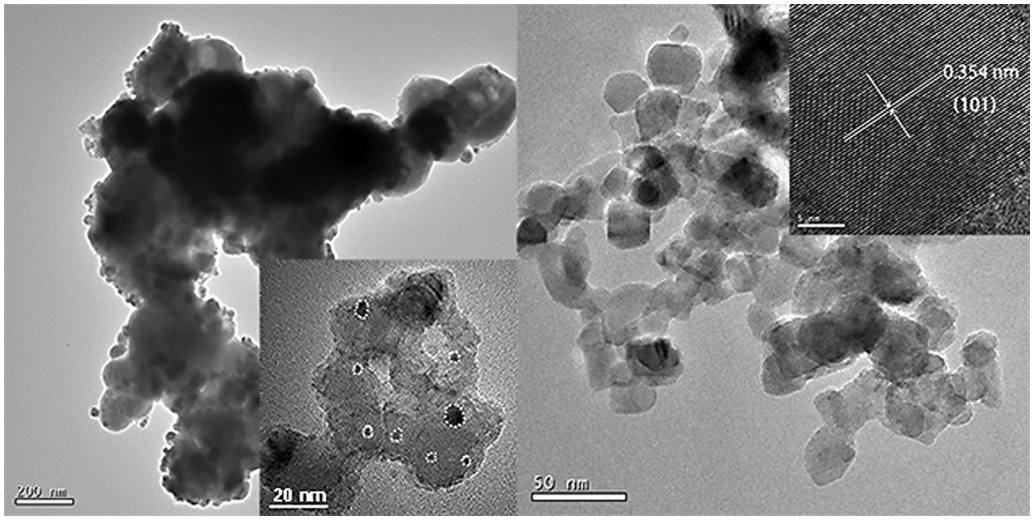

Fig. 2. TEM image of (a) self-corrosion 33 wt% Ag_3PO_4/TiO_2 compounds and (b) bare P25 TiO_2.

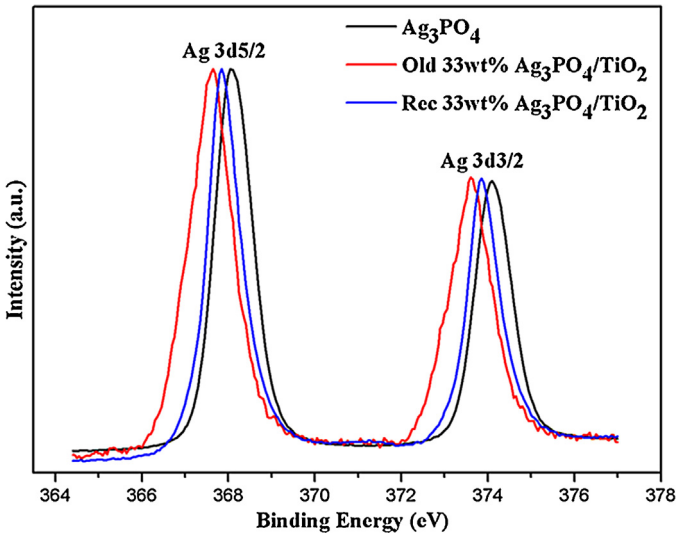

Fig. 3. XPS spectra of Ag 3d for self-corrosion, photo-corrosion 33 wt% Ag_3PO_4/TiO_2 and fresh Ag_3PO_4.

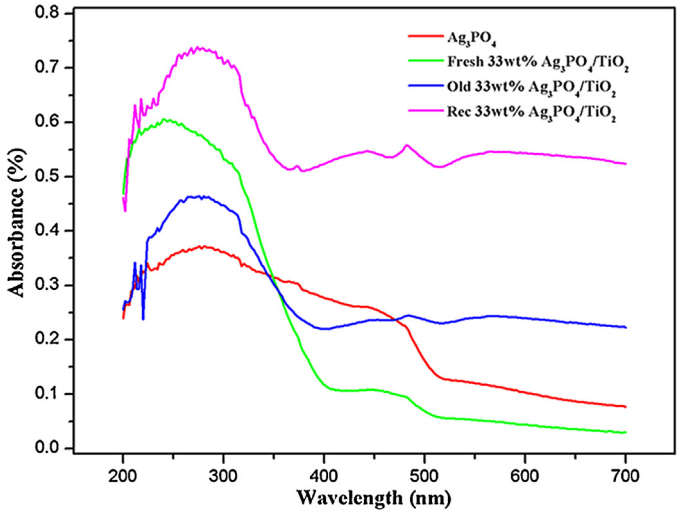

Fig. 4. UV–vis absorption spectra of fresh, self-corrosion, photo-corrosion 33 wt% Ag_3PO_4/TiO_2 and fresh Ag_3PO_4.

self-corrosion 33 wt% Ag_3PO_4/TiO_2. And these two peaks at 367.84 and 373.85 eV can be ascribed to the formation of Ag_2O particle on the surface of P25 TiO_2 according to the results reported by Chen et al. [18]. These results suggest that both self-corrosion and photo-corrosion can lead to various productions as well as the shift of XPS peaks in different degrees.

The XPS spectra of P 2p for the fresh Ag_3PO_4, self-corrosion 33 wt% Ag_3PO_4/TiO_2 and photo-corrosion 33 wt% Ag_3PO_4/TiO_2 are shown in Fig. S4. It can be seen that the peaks at about 133.53 eV both for self-corrosion 33 wt% Ag_3PO_4/TiO_2 and photo-corrosion 33 wt% Ag_3PO_4/TiO_2 are higher than that of the fresh Ag_3PO_4 at 132.56 eV. This indicates that the chemical environment around P in these compounds is altered and the significant decrease of intensity before normalization is due to the decrease of Ag_3PO_4 in these compounds and the formation of Ag_2O particles.

Therefore, according to the above information and results obtained from XPS spectra, it can be concluded that the chemical environment of Ag for self-corrosion and photo-corrosion Ag_3PO_4/TiO_2 compounds is both altered. Meanwhile, it is attributed to the decrease of Ag_3PO_4 in these compounds and the formation of Ag_xO ($x = 1,2$) and Ag_2O–Ag particle, respectively.

Fig. 4 shows the UV–vis absorption spectra of fresh, self-corrosion, photo-corrosion 33 wt% Ag_3PO_4/TiO_2 and fresh Ag_3PO_4, respectively. It can be seen that the absorption edges of self- and photo-corrosion Ag_3PO_4/TiO_2 compounds as well as fresh Ag_3PO_4/TiO_2 locate at around 520 and 420 nm. These edges corresponds to the feature absorption of bare Ag_3PO_4 (520 nm)

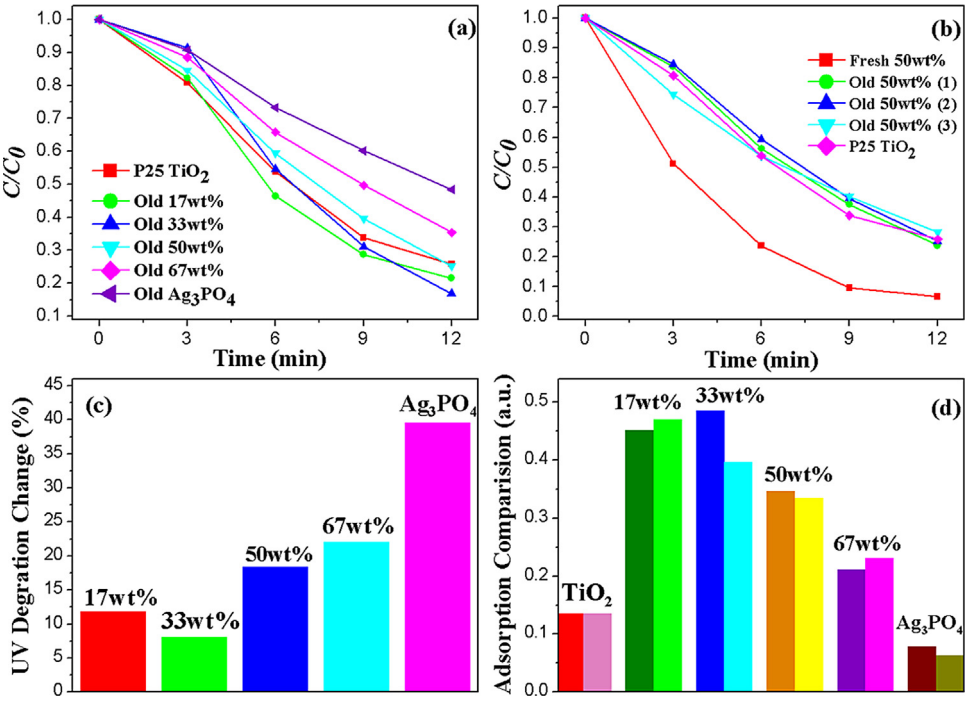

Fig. 5. (a) Photocatalytic performance under UV light irradiation of self-corrosion and fresh compounds; (b) photocatalytic activity dependence on kept time for 50 wt% Ag_3PO_4/TiO_2; (c) decreased degradation percentage for self-corrosion and fresh compounds; (d) adsorption capacity in dark of samples with different percentage of Ag_3PO_4. Left columns for fresh samples, and right columns for self-corrosion samples.

and P25 TiO_2 (420 nm) (Fig. S5). However, the absorption in the region of 400–700 nm is remarkably increased for the self-corrosion Ag_3PO_4/TiO_2 compounds (Fig. S6) due to the formation of Ag_xO ($x = 1, 2$) [17]. In contrast, the UV–vis spectrum of the photo-corrosion 33 wt% Ag_3PO_4/TiO_2 exhibits a wider and stronger absorption in the region of 400–700 nm than the fresh Ag_3PO_4 or self-corrosion Ag_3PO_4/TiO_2 compounds, which is resulted from the localized surface plasmon resonance absorption of Ag nanoparticles [15]. This result is in agreement with above conclusion obtained from XPS spectra.

3.3. Impact of self-corrosion on photocatalytic activity

In order to investigate the impact of the above changes on photocatalytic activity, the performance under UV light irradiation of the above self-corrosion samples compared with that of fresh compounds is conducted.

It can be seen in Fig. 5(a) that photocatalytic activity of self-corrosion Ag_3PO_4/TiO_2 samples in several compositions of Ag_3PO_4 are higher than that of self-corrosion bare Ag_3PO_4 and TiO_2, whereas that of 67 wt% Ag_3PO_4/TiO_2 decreased. This result follows the same regularity as fresh Ag_3PO_4/TiO_2 compounds (Fig S7). Fig. 5(b) reveals the photocatalytic activity dependence on kept time for 50 wt% Ag_3PO_4/TiO_2 (as a typical sample). It is noted that the photocatalytic activity of the self-corrosion samples kept for different time shows no obvious difference but lower than that of fresh Ag_3PO_4/TiO_2 compounds. This result suggests that the self-corrosion decreases the photocatalytic activities of Ag_3PO_4/TiO_2 compounds due to the loss of

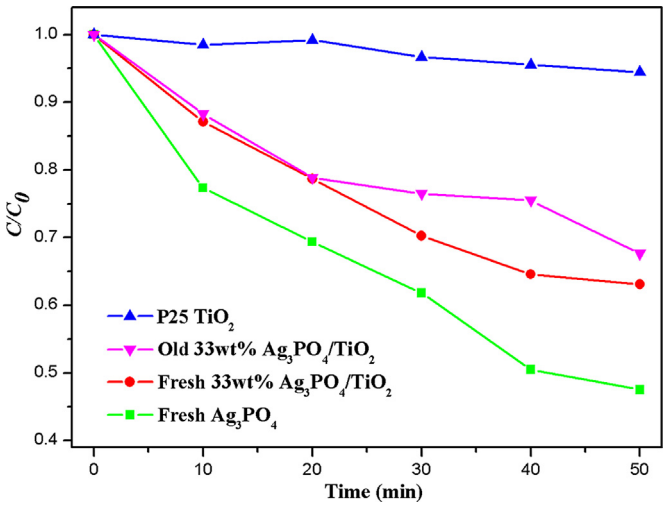

Fig. 6. Photocatalytic activities of fresh Ag_3PO_4, fresh 33 wt% Ag_3PO_4/TiO_2, self-corrosion 33 wt% Ag_3PO_4/TiO_2 and P25 TiO_2 under visible light irradiation.

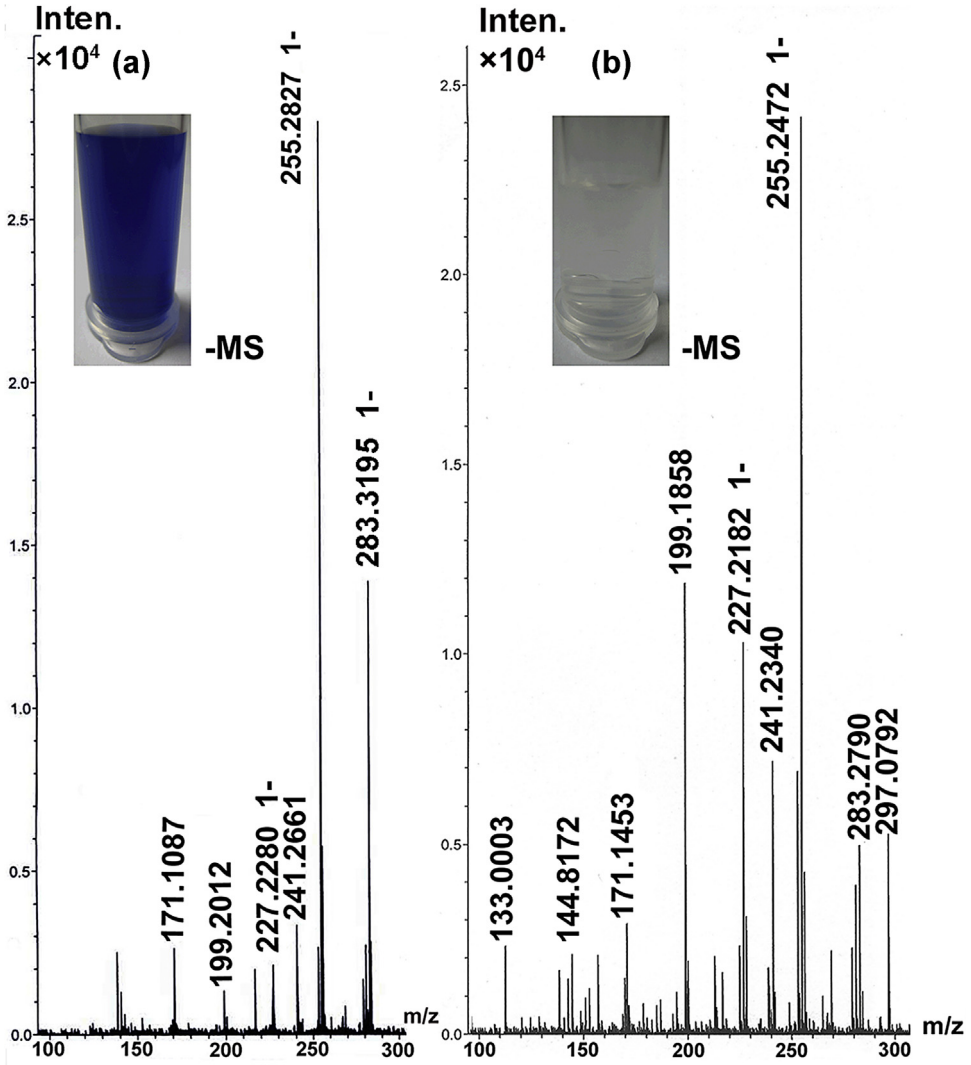

Fig. 7. Negative mass spectra of the major production before (a) and after (b) photodegradation.

Table 1
BET specific surface area of Ag_3PO_4/TiO_2 samples with different percentage of Ag_3PO_4.

BET (m^2/g)	Samples					
	P25	17 wt% Ag_3PO_4/TiO_2	33 wt% Ag_3PO_4/TiO_2	50 wt% Ag_3PO_4/TiO_2	67 wt% Ag_3PO_4/TiO_2	Ag_3PO_4
Fresh samples	46.2	46.1	35.3	28.5	19.7	1.7
Self-corrosion samples		44.3	42.2	29.1	20.0	

Ag_3PO_4 and the formation of Ag_xO ($x = 1, 2$). Moreover, the above decrease is independent on the self-corrosion time. Fig. 5(c) shows the decreased degradation percentage for self-corrosion samples compared with fresh compounds. The percentage is calculated by $((\Delta A_{fresh} - \Delta A_{self\text{-}corrosion})/\Delta A_{fresh})\%$, where ΔA_{fresh} and $\Delta A_{self\text{-}corrosion}$ are degradation percentage for fresh and self-corrosion samples. Thus, the smaller the percentage is, the more stable the sample is. It can be seen from Fig. 5(c) that these decreased degradation percentages are 11.8% (17 wt%), 8.0% (33 wt%), 18.4% (50 wt%), 22.0% (67 wt%) and 39.5% (bare Ag_3PO_4), respectively. It means that the 33 wt% Ag_3PO_4/TiO_2 kept in dark for 5 days still maintains a high photocatalytic activity. However, bare Ag_3PO_4 decreases about 39.5%, which is worse than that of Ag_3PO_4/TiO_2 compounds. These results indicate that the photocatalytic activities of Ag_3PO_4/TiO_2 compounds are more stable than that of bare Ag_3PO_4 after self-corrosion, especially for the performance of 33 wt% Ag_3PO_4/TiO_2.

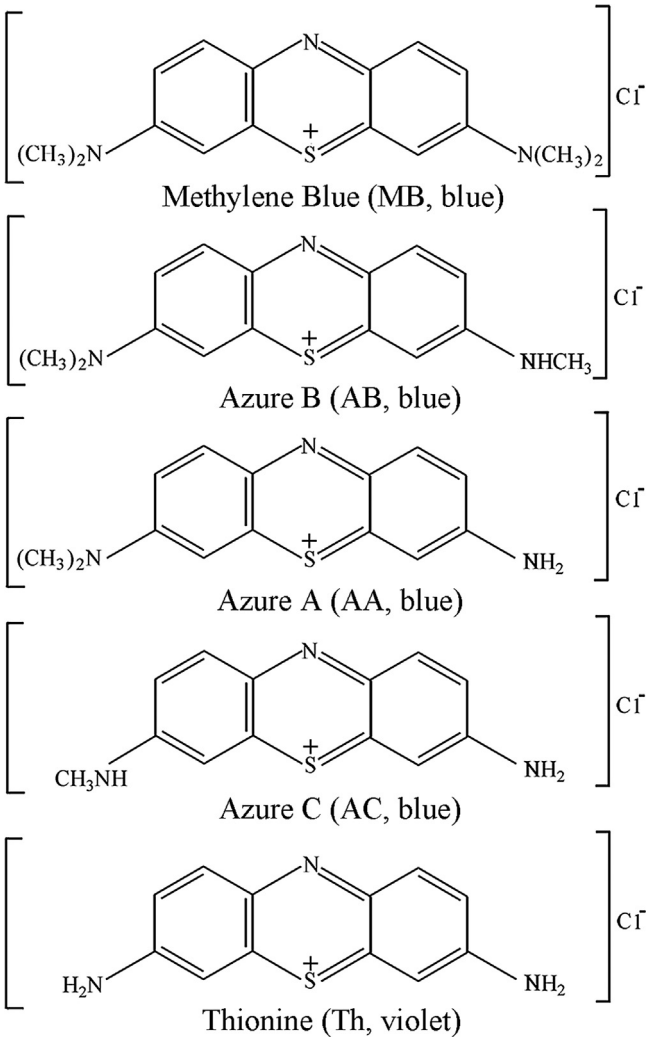

Fig. 8. Chemical structures of MB and of related demethylated intermediates during photocatalytic degradation process.

Fig. 5(d) depicts the adsorption capacity of TiO_2, 17 wt% Ag_3PO_4/TiO_2, 33 wt% Ag_3PO_4/TiO_2, 50 wt% Ag_3PO_4/TiO_2, 67 wt% Ag_3PO_4/TiO_2 and bare Ag_3PO_4 in dark, respectively. The left and right columns represent the adsorption capacity of fresh and self-corrosion samples. Here, the adsorption ratio is calculated by $(A_{adsorption}/A_0)\%$, where A_0 is the initial absorption of MB solution tested by UV–vis spectroscopy, $A_{adsorption}$ is the absorption of MB solution after adsorption process. It can be seen that the Ag_3PO_4/TiO_2 compounds, no matter fresh or self-corrosion samples, show higher adsorption ratio than those of P25 TiO_2 and Ag_3PO_4, especially for 17 wt% Ag_3PO_4/TiO_2 and 33 wt% Ag_3PO_4/TiO_2 (corresponding to 45.1%, 48.5% for fresh compounds; 47.0%, 39.6% for self-corrosion compounds). Furthermore, the adsorption capacities change slightly between fresh and self-corrosion Ag_3PO_4/TiO_2 compounds. According to the above results, it can be concluded that the adsorption capacity plays a significant role in determining photocatalytic activities of Ag_3PO_4/TiO_2 compounds under UV light irradiation. It is the strong adsorption capacity that makes the higher photocatalytic activities for fresh and self-corrosion Ag_3PO_4/TiO_2 compounds than bare Ag_3PO_4 and TiO_2. Meanwhile, since the advantage of adsorption capacity is not changed, the photocatalytic activities for Ag_3PO_4/TiO_2 compounds are independent on self-corrosion time and more stable than that of bare Ag_3PO_4. In addition, the values of BET S.S.A. of the above samples are listed in Table 1. It can be seen that the higher the percentage of Ag_3PO_4 in compound is, the bigger the BET S.S.A. is. Meanwhile, it is almost the same values of BET S.S.A. for fresh and self-corrosion samples, well within the margin of error. This result indicates that the strong adsorption capacity does not have a close relation with the values of BET S.S.A. for Ag_3PO_4/TiO_2 samples.

Fig. 6 shows the photocatalytic activities of fresh Ag_3PO_4, fresh 33 wt% Ag_3PO_4/TiO_2, self-corrosion 33 wt% Ag_3PO_4/TiO_2 and P25 TiO_2 under visible light irradiation, respectively. It can be seen that fresh Ag_3PO_4 shows the highest photocatalytic activity while P25 TiO_2 can hardly decompose MB solution. Thus, the amount of Ag_3PO_4 in Ag_3PO_4/TiO_2 compounds almost determines the photocatalytic activities under visible light irradiation. It is confirmed that fresh Ag_3PO_4/TiO_2 compounds show lower photocatalytic activity than bare Ag_3PO_4 owing to the lower amount of Ag_3PO_4. Meanwhile, the decrease of Ag_3PO_4 in self-corrosion Ag_3PO_4/TiO_2 compounds leads to the worse performance, though the absorption increases due to the formation of Ag_xO ($x = 1, 2$) particles.

In summary, the impact of self-corrosion on photocatalytic activity is discussed for Ag_3PO_4/TiO_2 compounds. Since the key factors of photocatalytic activities are different under UV and visible light irradiation, the impacts of self-corrosion for Ag_3PO_4/TiO_2 on photocatalytic activities are different.

3.4. MS studies for intermediates analysis and degradation mechanism

Further analysis of product formation was done by MS studies of the degradation intermediate products. Compared with negative mass spectra (−MS) peaks of the parent molecule in Fig. 7(a), it can be seen from Fig. 7(b) that the MB cation molecule peak intensity decreases at $m/z = 284$ amu after UV light irradiation for 15 min in the presence of self-corrosion 33 wt% Ag_3PO_4/TiO_2. In addition, the spectrum of Fig. 7(b) shows the increase of peaks

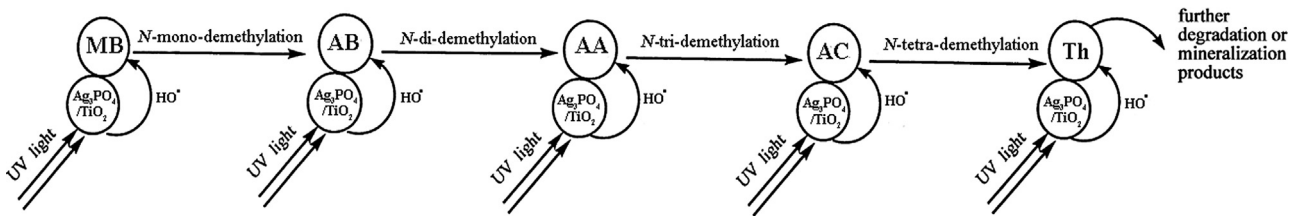

Fig. 9. Scheme depicting the demethylation of MB and the dynamic equilibrium of MB and demethylated species between the bulk solution and the Ag_3PO_4/TiO_2 particle surface during the photodegradation of MB.

intensity at m/z = 270, 256, 242, and 228 amu. These peaks correspond to Azure B (AB), Azure A (AA), Azure C (AC), and thionin (Th), respectively, as shown in Fig. 8. According to previous work, these fragment ion species are due to the demethylation cleavage during the photocatalytic degradation, which are in agreement with the intermediate products degraded by bare TiO_2 as reported in literatures [19–21]. Meanwhile, the demethylation cleavage and further degradation can be confirmed by positive mass spectra (+MS) (FigS8). In addition, the result is the same in the presence of fresh 33 wt% Ag_3PO_4/TiO_2 (Fig. S9). These results indicate that it is the same degradation process for self-corrosion and fresh Ag_3PO_4/TiO_2 as well as bare TiO_2.

Furthermore, the photocatalytic degradation of MB solution is well documented in the literature and is believed to involve •OH radicals which are produced in a series of reactions [19,20]. These radicals then attack the MB cation molecule and cause it to degrade as shown in Fig. 9 [19]. Thus, the integrating Ag_3PO_4 with TiO_2 facilitates the electron–hole separation and increases •OH radicals production and thereby improves the photocatalytic activity [13].

However, something is still unknown: what generates the strong adsorption capacity after simple physical mixing Ag_3PO_4 and TiO_2, and how it influence the photocatalytic activity, which will be discussed later in our next work.

4. Conclusion

The phenomenon of "self-corrosion" was first observed in the simple physical mixed Ag_3PO_4/TiO_2 compounds. It is found that the chemical environment of Ag is altered due to both the self-corrosion and photo-corrosion in Ag_3PO_4/TiO_2 compounds compared with that in bare Ag_3PO_4. But the corrosion degree is different for the slight difference of the chemical environment between self-corrosion and photo-corrosion for Ag. Meanwhile, the color-change of Ag_3PO_4/TiO_2 compounds in dark is due to the formation of Ag_xO (x = 1, 2) instead of Ag particles. Furthermore, it is the strong adsorption capacity that determines photocatalytic activities of Ag_3PO_4/TiO_2 compounds under UV light irradiation, which is almost independent on the self-corrosion. In contrast, it is the amount of visible-light-response Ag_3PO_4 in Ag_3PO_4/TiO_2 compounds that mainly determines the photocatalytic activities under visible light irradiation, which is highly relevant to the self-corrosion. Finally, it can be confirmed by MS that it is the same degradation process for self-corrosion and fresh Ag_3PO_4/TiO_2 as well as bare TiO_2, and the integrating Ag_3PO_4 with TiO_2 facilitates the electron–hole separation and increases •OH radicals production and thereby improves the photocatalytic activity.

Acknowledgments

This work was supported by the National Nature Science Young Foundation of China (No. 10904057), the International Sci. & Tech. Cooperation Foundation of Gansu Provincial, China (Grant No. 1304WCGA177), the Fundamental Research Funds for Central Universities (No. lzujbky-2013-28), Technology Foundation for Selected Overseas Chinese Scholar (Department of Human Resources and Social Security of Gansu Province), the Basic Scientific Research Business Expenses of the Central University, and Open Project of Key Laboratory for Magnetism and Magnetic Materials of the Ministry of Education, Lanzhou University (No. LZUMMM2014008).

Appendix A. Supplementary data

Supplementary data associated with this article can be found, in the online version, at http://dx.doi.org/10.1016/j.apcatb.2014.04.031.

References

[1] S. Anandan, A. Vinu, T. Mori, N. Gokulakrishnan, P. Srinivasu, V. Murugesan, K. Ariga, Catal. Commun. 8 (2007) 1377–1382.
[2] (a) H.H. Li, S. Yin, Y.H. Wang, T. Sato, Appl. Catal. B 132–133 (2013) 487–492; (b) H.H. Li, S. Yin, T. Sato, Appl. Catal. B 106 (2011) 586–591.
[3] C.F. Lin, C.H. Wu, Z.N. Onn, J. Hazard. Mater. 154 (2008) 1033–1039.
[4] X. Chen, S. Shen, L. Guo, S. Mao, Chem. Rev. 110 (2010) 6503.
[5] Y. Liu, L. Fang, H. Lu, L. Liu, H. Wang, C. Hu, Catal. Commun. 17 (2011) 200–204.
[6] (a) B.T. Liu, Y.J. Huang, Y. Wen, L.J. Du, W. Zeng, J. Mater. Chem. 22 (2012) 7484–7491; (b) B.T. Liu, L.L. Peng, J. Alloys Compd. 571 (2013) 145–152.
[7] Z. Yi, J. Ye, N. Kikugawa, T. Kako, S. Ouyang, H. Stuart-Williams, H. Yang, J. Cao, W. Luo, Z. Li, Nat. Mater. 9 (2010) 559–564.
[8] Y. Bi, S. Ouyang, N. Umezawa, J. Cao, J. Ye, J. Am. Chem. Soc. 133 (2011) 6490–6492.
[9] Y. Bi, H. Hu, S. Ouyang, G. Lu, J. Cao, J. Ye, Chem. Commun. 48 (2012) 3748–3750.
[10] H. Wang, Y. Bai, J. Yang, X. Lang, J. Li, L. Guo, Chem. Eur. J. 18 (2012) 5524–5529.
[11] Y. Bi, S. Ouyang, J. Cao, J. Ye, Phys. Chem. Chem. Phys. 13 (2011) 10071–10075.
[12] S.B. Rawal, S.D. Sung, W.I. Lee, Catal. Commun. 17 (2012) 131–135.
[13] W. Yao, B. Zhang, C. Huang, C. Ma, X. Song, Q. Xu, J. Mater. Chem. 22 (2012) 4050–4055.
[14] H. Zhang, G. Wang, D. Chen, X. Lv, J. Li, Chem. Mater. 20 (2008) 6543–6549.
[15] Y.P. Liu, L. Fang, H.D. Lu, Y.W. Li, C.Z. Hua, H.G. Yu, Appl. Catal. B 115–116 (2012) 245–252.
[16] I.M. Arabatzi, T. Stergiopoulos, M.C. Bernard, D. Labou, S.G. Neophytides, P. Falaras, Appl. Catal. B 42 (2003) 187–201.
[17] X.F. Wang, S.F. Li, H.G. Yu, J.G. Yu, S.W. Liu, Chem. Eur. J. 17 (2011) 7777–7780.
[18] F.T. Chen, Z. Liu, Y. Liu, P.F. Fang, Y.Q. Dai, Chem. Eng. J. 221 (2013) 283–291.
[19] T.Y. Zhang, T. Oyama, A. Aoshima, H. Hidaka, J.C. Zhao, N. Serpone, J. Photochem. Photobiol. A: Chem. 140 (2001) 163–172.
[20] M.A. Rauf, M.A. Meetani, A. Khaleel, A. Ahmed, Chem. Eng. J. 157 (2010) 373–378.
[21] A. Orendorz, C. Ziegler, H. Gnaser, Appl. Surf. Sci. 255 (2008) 1011–1014.